# Nonreciprocal Directional Dichroism in Magnetoelectric Spin Glass

Y. Sawada,[1] S. Kimura,[1] K. Watanabe,[1] Y. Yamaguchi,[2] T. Arima,[3] and T. Kimura[3]
[1]Institute for Materials Research, Tohoku University, Sendai 980-8577, Japan
[2]Division of Materials Physics, Graduate School of Engineering Science, Osaka University, Toyonaka 560-8531, Japan
[3]Department of Advanced Materials Science, University of Tokyo, Kashiwa 277-8561, Japan

(Received 11 April 2022; revised 29 August 2022; accepted 18 October 2022; published 15 November 2022)

Optical absorption spectra in the visible and near-infrared light were measured for magnetoelectric spin glass $Ni_{0.4}Mn_{0.6}TiO_3$ under various field-cooled conditions. Despite the absence of long-range magnetic-dipole order, this spin-glass system exhibits nonreciprocal directional dichroism (NDD) at zero external field after a magnetoelectric field-cooled procedure. This result is distinct from previous studies on NDD in systems with magnetic toroidal moments induced either by long-range magnetic-dipole order or by applying crossed electric and magnetic fields. The present Letter conclusively demonstrates that the observed NDD originates from magnetoelectrically induced ferroic order of magnetic toroidal moments without conventional magnetic-dipole order.

DOI: 10.1103/PhysRevLett.129.217201

Nonreciprocal directional dichroism (NDD)—change in optical absorption by reversing the direction of light propagation—is one of the nonreciprocal optical phenomena that rectify electromagnetic wave propagation and have contributed greatly to device applications such as isolators [1]. Though there have been various approaches to nonreciprocal light propagation [2–4], recent research developments on multiferroics revealed that materials exhibiting a magnetoelectric (ME) effect are favorable for achieving gigantic NDD [5–8]. The ME effect is a cross-coupling phenomenon between electricity and magnetism, in which electric polarization $\boldsymbol{P}$ (magnetization $\boldsymbol{M}$) is induced by a static magnetic field $\boldsymbol{H}$ (electric field $\boldsymbol{E}$). The optical magnetoelectric (OME) effect is an extension of the ME effect to the frequency region, that is, the ME effect induced by an oscillating electric or magnetic field of electromagnetic wave [5]. From the symmetry point of view, both the space-inversion and time-reversal symmetries must be broken for the presence of the linear (O)ME effect. These symmetry requirements are also applied to nonreciprocal phenomena where physical quantities change upon a reversal of the direction of wave propagation [5,6]. When an electromagnetic wave with the angular frequency of $\omega$ propagates through a medium that breaks these symmetries with the cross product of $\boldsymbol{P}$ and $\boldsymbol{M}$ along $(\boldsymbol{P}\times\boldsymbol{M})$, its oscillating magnetic field $(\boldsymbol{H}^{\omega})$ induces an oscillating electric dipole moment $(\boldsymbol{P}^{\omega}_{H})$ which interferes with an oscillating electric dipole moment $(\boldsymbol{P}^{\omega}_{E})$ induced by the oscillating electric field $(\boldsymbol{E}^{\omega})$ of the electromagnetic wave. This OME effect gives rise to NDD, because the constructive interference between $\boldsymbol{P}^{\omega}_{H}$ and $\boldsymbol{P}^{\omega}_{E}$ changes to be destructive by reversing the propagation vector $\boldsymbol{k}$. Thus, NDD can be expected due to a component of the refractive index with the form $\delta n = \gamma \boldsymbol{k}\cdot(\boldsymbol{P}\times\boldsymbol{M})$ [$\gamma$ = const], whose sign changes by a reversal of $\boldsymbol{k}$ [9]. In fact, most of the experimental studies on NDD were reported for materials with finite $(\boldsymbol{P}\times\boldsymbol{M})$, such as materials in crossed $\boldsymbol{E}$ and $\boldsymbol{H}$ [9,10], polar materials in $\boldsymbol{H}$ [11–13], magnetoelectrics in $\boldsymbol{H}$ [14–16], and polar magnets with spontaneous $\boldsymbol{P}$ and $\boldsymbol{M}$ [17,18].

However, even in the absence of $(\boldsymbol{P}\times\boldsymbol{M})$, NDD can be induced by the presence of ME multipole moments such as magnetic toroidal and quadrupole moments which lead to off-diagonal linear ME effects [19–22]. The magnetic toroidal moment is defined as $\boldsymbol{t}\propto\Sigma_n \boldsymbol{r}_n\times\boldsymbol{S}_n$, where $\boldsymbol{r}_n$ denotes a position vector of spin $\boldsymbol{S}_n$ at $n$ site and is odd under both the space-inversion and time-reversal transformations. Most typically, $\boldsymbol{t}$ is generated by head-to-tail arrangements of spins, namely, a spin vortex. Figure 1(a) illustrates $\boldsymbol{t}$ along the $z$ axis with an antisymmetric off-diagonal ME component $\alpha_{xy}=-\alpha_{yx}$. When $\boldsymbol{k}$ is parallel or antiparallel to $\boldsymbol{t}$, the necessary and sufficient symmetry condition for finite NDD is fulfilled [6]. Because $\boldsymbol{t}$ is closely

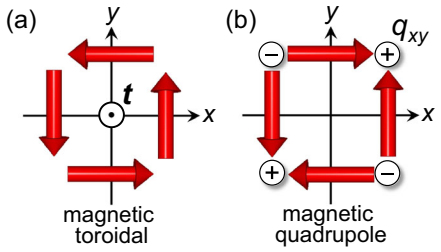


FIG. 1. Schematic illustrations of representative magnetoelectric multipole moments. Spin configurations inducing finite $t_z$-type magnetic toroidal (a) and $q_{xy}$-type magnetic quadrupole (b) moments with the off-diagonal ME coefficients. Red arrows denote spins.

 

coupled with $(\boldsymbol{E}\times\boldsymbol{H})$, offering a contribution to the free energy $F_t \propto -\boldsymbol{t}\cdot(\boldsymbol{E}\times\boldsymbol{H})$, $\boldsymbol{P}$ (or $\boldsymbol{M}$) is induced by the antisymmetric ME effect as $\boldsymbol{P}\propto -\boldsymbol{t}\times\boldsymbol{H}$ (or $\boldsymbol{M}\propto\boldsymbol{t}\times\boldsymbol{E}$) [21]. Since $(\boldsymbol{P}_H^{\omega}\times\boldsymbol{H}^{\omega})$ ascribed to the magnetic toroidal moment is independent of the polarization angle of the incident light, NDD due to $\boldsymbol{t}$ is independent of light polarization. Recently, NDD in the visible and near-infrared light regions has been reported for ME antiferromagnetic materials with finite $\boldsymbol{t}$ but not $(\boldsymbol{P}\times\boldsymbol{M})$ (e.g., $LiCoPO_4$ [23], $MnTiO_3$ [24], and $Bi_2CuO_4$ [25]). Furthermore, nonreciprocal optical responses can also arise from magnetic quadrupole moment ($q_{ij}\propto\Sigma_n[r_{ni}S_{nj}+r_{ni}S_{nj}-\frac{2}{3}\delta_{ij}\boldsymbol{r}_n\cdot\boldsymbol{S}_n]$, where $i$ and $j$ denote the $x$, $y$, or $z$ axis). Figure 1(b) illustrates a $q_{xy}$-type quadrupole moment with an off-diagonal symmetric ME component $\alpha_{xy}=\alpha_{yx}$. In contrast to the toroidal case, $(\boldsymbol{P}_H^{\omega}\times\boldsymbol{H}^{\omega})$ due to the magnetic quadruple depends on the angle of the incident light polarization. This anisotropy results in the so-called nonreciprocal linear dichroism (NLD) [26]. Indeed, NLD has recently been observed in ME antiferromagnetic $Pb(TiO)Cu_4(PO_4)_4$ with finite magnetic quadrupole moment but not $(\boldsymbol{P}\times\boldsymbol{M})$ [27].

In this Letter, we investigate nonreciprocal optical responses in the visible and near-infrared regions for spin glass $Ni_{0.4}Mn_{0.6}TiO_3$, which shows off-diagonal and antisymmetric ME effects despite the absence of long-range magnetic order. We demonstrate that this ME spin glass shows NDD even in the absence of external fields. This result implies that the spin frozen state of the ME spin glass can host components of magnetic toroidal moments and is distinct from the above-mentioned former studies on systems with the ME multipole moments induced either by long-range magnetic order or by applying $(\boldsymbol{E}\times\boldsymbol{H})$.

The material focused on this Letter, $Ni_{0.4}Mn_{0.6}TiO_3$ (NMTO), crystallizes in the centrosymmetric ilmenite structure in which magnetic $Ni^{2+}$ and $Mn^{2+}$ ions are randomly distributed on a honeycomb lattice [Fig. 2(a)]. As a result, NMTO exhibits a spin glass transition at $T_{SG}\approx 9.5$ K and is classified as an $XY$-like spin glass with an easy-plane anisotropy [28–30]. Moreover, the spin glass phase exhibits an antisymmetric linear ME effect with glasslike behaviors such as strong field-cooled condition dependence [30,31]. Figure 2(b) displays temperature ($T$) profiles of $\boldsymbol{P}$ ($\|[1\bar{1}0]$ in the hexagonal setting) at 9 T ($\|[110]$) and 0 MV m$^{-1}$ in a single crystal of NMTO after cooling the sample at a fixed magnetic field (9 T) and various electric fields ranging from 0 to 0.5 MV m$^{-1}$. Prior to the respective measurements, $\boldsymbol{E}$ along $[1\bar{1}0]$ and $\boldsymbol{H}$ along [110] were applied at 20 K. Subsequently, the sample was cooled to 2 K while holding the $\boldsymbol{E}$ and $\boldsymbol{H}$ (ME cooling). The data clearly show the strong field-cooled condition dependence below $T_{SG}$. It is notable that the linear ME effect appears in the centrosymmetric compound without long-range magnetic order because the linear ME effect requires broken space-inversion and time-reversal symmetries.

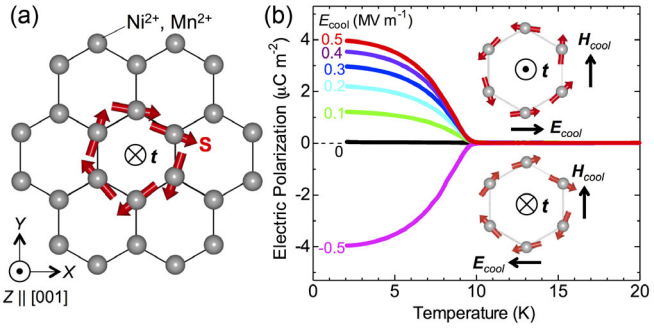


FIG. 2. Glassy feature of magnetoelectricity in ilmenite-type $Ni_{0.4}Mn_{0.6}TiO_3$. (a) Schematic crystal structure of $Ni_{0.4}Mn_{0.6}TiO_3$ projected along [001] (hexagonal setting). Only sites at which magnetic ions sit are depicted. Randomly distributed $Ni^{2+}$ and $Mn^{2+}$ ions form stacked honeycomb lattices. Red arrows denote randomly frozen spins aligned within the $XY$ plane on the respective magnetic ions, which generate a finite toroidal moment $\boldsymbol{t}$. (b) Temperature profiles of electric polarization measured at 9 T and 0 MV m$^{-1}$ after cooling the sample at a fixed cooling magnetic field (9 T) and various cooling electric fields ranging from 0 to 0.5 MV m$^{-1}$. The insets of (b) show expected configurations of $\boldsymbol{t}$ after the respective ME-cooled conditions.

Considering the antisymmetric and glass natures of the linear ME effect, its origin has been discussed in terms of a magnetoelectrically controlled frozen state of the toroidal moment [30,31]. As illustrated in Fig. 2(a) and the insets of Fig. 2(b), local spin textures in the $XY$-like spin glass with the honeycomb lattice generate local toroidal moments either with $\pm\boldsymbol{t}$ along the [001] direction [32]. It was suggested that the presence of $(\boldsymbol{E}\times\boldsymbol{H})\|[001]$ during the spin freezing process polarizes net $\boldsymbol{t}$ along [001] to gain the free energy, which can cause the observed ME effect in the spin glass phase. Thus, we anticipate that NMTO cooled at finite $(\boldsymbol{E}\times\boldsymbol{H})$ exhibits NDD ascribed to the spin frozen state with the magnetoelectrically polarized toroidal moment.

To examine NDD in the spin glass phase of NMTO, we measured optical absorption spectra in the visible and near-infrared light regions by using a high-field optical spectroscopy system [33]. The light was illuminated along the [001] direction, i.e., $\boldsymbol{k}\|[001]$. Details of the experiments are described in Supplemental Material [34]. Figure 3(a) shows a representative absorption ($A$) spectrum taken at 4.2 K in the absence of $\boldsymbol{E}$ and $\boldsymbol{H}$. As indicated by thick arrows, the spectrum exhibits three peaks at around 11 900, 13 200, and 23 000 cm$^{-1}$ though that around 23 000 cm$^{-1}$ is saturated. From the comparison with the optical spectra of Ni complexes [35], we assign the absorption peaks around 11 900 and 23 000 cm$^{-1}$ to spin-allowed $d$-$d$ transitions of $Ni^{2+}$ and that around 13 200 cm$^{-1}$ to a spin-forbidden $d$-$d$ transition of $Ni^{2+}$. Prior to the respective NDD measurements, we applied crossed $\boldsymbol{E}$ and $\boldsymbol{H}$ in the (001) plane of NMTO at 20 K ($>T_{SG}$), as depicted in the

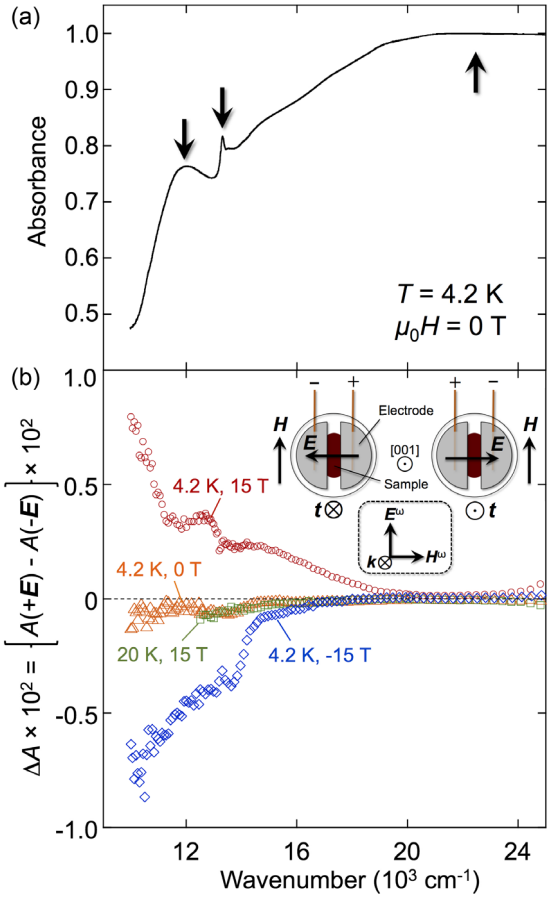


FIG. 3. Spectra of nonreciprocal directional dichroism (NDD) of $Ni_{0.4}Mn_{0.6}TiO_3$ in the visible and near-infrared light regions. (a) Absorption spectra taken at 4.2 K with the incident light propagating along [001] (hexagonal setting) in the absence of external field $\boldsymbol{E}$ and magnetic field $\boldsymbol{H}$. Thick arrows in (a) indicate peak structures in the spectrum. (b) The difference between the absorption spectra measured at opposite electric fields ($\pm\boldsymbol{E} = \pm 0.4$ MV m$^{-1}$), $\Delta A\{= [A(+\boldsymbol{E}) - A(-\boldsymbol{E})]\}$, corresponds to NDD. Open green squares show the data measured in $\boldsymbol{H}$ of 15 T at 20 K (paramagnetic phase). Open orange triangles, red circles, and blue diamonds denote the data measured in 0, +15, and −15 T, respectively, at 4.2 K (spin glass phase). Prior to the measurements in the spin glass phase, $\boldsymbol{E}$ and $\boldsymbol{H}$ were first set to the measurement conditions at 20 K. Subsequently, the sample was cooled down to 4.2 K. The inset illustrates the experimental setup. Crossed $\boldsymbol{E}$ and $\boldsymbol{H}$ were applied in the direction parallel to the (001) plane, and the propagation vector of light $\boldsymbol{k}$ is along [001]. All the data shown in (b) were taken by using the polarized light whose polarization geometry is illustrated in the inset. $\boldsymbol{E}^{\omega}$ and $\boldsymbol{H}^{\omega}$ denote the oscillating electric-field and magnetic-field components of the light, respectively.

inset of Fig. 3(b) (ME cooling). Then, the sample was set to the measurement temperature while holding the applied $\boldsymbol{E}$ and $\boldsymbol{H}$. Thus, measurements in the spin glass phase ($<T_{SG}$) were done after ME cooling, i.e., cooling in the presence of finite ($\boldsymbol{E} \times \boldsymbol{H}$). Instead of reversing the light propagation, i.e., the sign of $\boldsymbol{k}$, we obtained NDD by reversing the sign of $\boldsymbol{E}$ during the ME cooling process, which will cause a sign reversal of $\boldsymbol{t}$. Thus, NDD is detected as the difference between two optical absorption spectra, $\Delta A\{= [A(+\boldsymbol{E}) - A(-\boldsymbol{E})]\}$, obtained after the ME cooling processes with $\pm\boldsymbol{E}$ ($= \pm 0.4$ MV m$^{-1}$).

Figure 3(b) displays $\Delta A$ obtained using linearly polarized light under several conditions in terms of $\boldsymbol{H}$ and $T$. The polarization geometry of incident light is illustrated in the inset. For all the data shown in Fig. 3(b), $\boldsymbol{E}$ and $\boldsymbol{H}$ were first set to the measurement conditions at 20 K. Subsequently, the sample was cooled to a measurement temperature. When $\Delta A$ is measured in the paramagnetic phase ($T = 20$ K $> T_{SG}$) at finite ($\boldsymbol{E} \times \boldsymbol{H}$), no substantial signal is observed in the entire wave number region studied here [green squares in Fig. 3(b)]. Moreover, when $\Delta A$ is taken in the spin glass phase ($T = 4.2$ K $< T_{SG}$) after cooling the sample only in $\boldsymbol{E}$ but not in $\boldsymbol{H}$, that is, in the absence of ($\boldsymbol{E} \times \boldsymbol{H}$), the data almost overlap those obtained at 20 K and show no NDD [orange triangles in Fig. 3(b)]. In contrast, for the data in the spin glass phase ($T = 4.2$ K $< T_{SG}$) with finite ($\boldsymbol{E} \times \boldsymbol{H}$),$|\Delta A|$ develops below 16 000 $\sim$ 20 000 cm$^{-1}$ and reaches up to 0.8% at around 10, 000 cm$^{-1}$ [red circles and blue diamonds in Fig. 3(b)]. Thus, NDD develops only in the spin glass phase at finite ($\boldsymbol{E} \times \boldsymbol{H}$) after the ME cooling. Furthermore, by comparing the data at 4.2 K in magnetic fields of +15 T (red circles) and −15 T (blue diamonds), it is obvious that the sign of $\Delta A$ is reversed by the sign change of $\boldsymbol{H}$. These results are well explained by considering that the sign of net toroidal moment which depends on that of ($\boldsymbol{E} \times \boldsymbol{H}$) is reversed by a reversal of either $\boldsymbol{E}$ or $\boldsymbol{H}$.

Next, to examine whether the observed directional dichroism in NMTO is purely due to toroidal moment without ($\boldsymbol{P} \times \boldsymbol{M}$), we turn off both the external electric and magnetic fields after the ME cooling. Experimental procedures prior to the measurements are schematically drawn in Fig. 4(a). After the sample was cooled down to 4.2 K in finite $\boldsymbol{E}$ and $\boldsymbol{H}$, only $\boldsymbol{E}$ was removed (red open circle) or both $\boldsymbol{E}$ and $\boldsymbol{H}$ were removed (green filled triangle) before the measurements. Figure 4(c) displays the results measured in a magnetic field of 15 T (red open circles) and at zero magnetic field (green filled triangles). Here $\Delta A$ is the difference between the absorption spectra measured at 4.2 K after cooling the sample in opposite cooling electric fields $\pm E_{cool}$, $\Delta A\{= [A(+E_{cool}) - A(-E_{cool})]\}$. Surprisingly, these two data well coincide with each other, which means that the cooling condition is more critical for NDD than the measurement condition. As shown in Fig. 4(b), $\boldsymbol{P}$ in NMTO becomes zero in the absence of $\boldsymbol{H}$ even after the ME cooling [30]. [Note that the static ME effect cannot be detected with measurements of $\boldsymbol{P}$ in the absence of $\boldsymbol{H}$. In other words, the absence of $\boldsymbol{P}$ at $\boldsymbol{H} = 0$ in Fig. 4(b) does not mean the disappearance of the ME tensor for the static ME effect.] Thus, although $\boldsymbol{M}$ slightly remains due to the long relaxation time inherent in spin glasses,

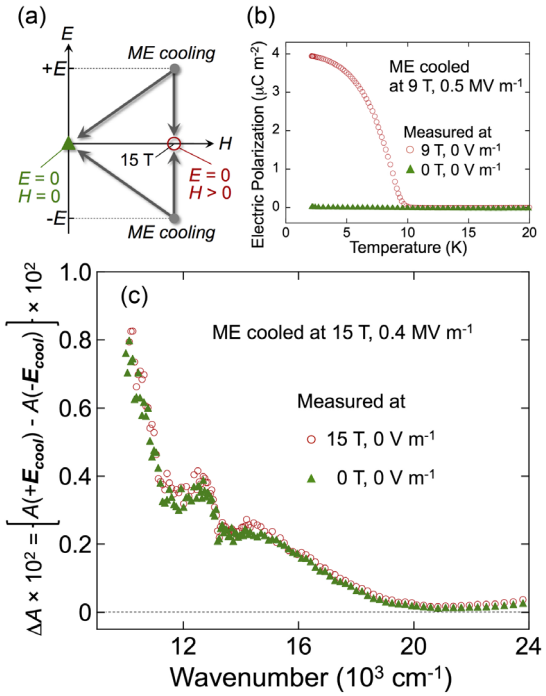


FIG. 4. Nonvolatile feature of nonreciprocal directional dichroism (NDD) in $Ni_{0.4}Mn_{0.6}TiO_3$. (a) Schematic representation of magnetoelectric (ME) cooling procedure done prior to the measurements shown in (b) and (c). (b) Temperature dependence of electric polarization $\boldsymbol{P}$ measured in the absence of electric field $\boldsymbol{E}$ at magnetic fields $\boldsymbol{H}$ of 0 T (green filled triangles) and 9 T (red open circles). (c) The difference between the absorption spectra measured at 4.2 K after cooling the sample in opposite cooling electric fields $\pm E_{\mathrm{cool}}$. All the data shown in (b) and (c) were taken in the absence of $\boldsymbol{E}$ during the measurements. Before the measurements, ME cooling was done with a finite magnetic field [$H_{\mathrm{cool}}$ of 9 for (b) and 15 T for (c)] and a finite electric field [$E_{\mathrm{cool}}$ of 0.5 for (b) and 0.4 MV m$^{-1}$ for (c)]. Red open circles show the data measured in a finite magnetic field [9 for (b) and 15 T for (c)], while green filled triangles denote the data measured at zero magnetic field. The NDD data at 0 T was taken after the magnetic field was swept from 15 to 0 T at a rate of 0.017 T sec$^{-1}$. These data demonstrate that NDD is observed even at $|\boldsymbol{P} \times \boldsymbol{M}| = 0$.

$(\boldsymbol{P} \times \boldsymbol{M})$ is zero in our measurement of $\Delta A$ at $|\boldsymbol{E}| = |\boldsymbol{H}| = 0$ [green triangles in Fig. 4(c)]. Therefore, our observation of NDD at zero electric and magnetic fields clearly demonstrates breakings of space-inversion and time-reversal symmetries in the ME-cooled spin frozen state which remains even after $\boldsymbol{E}$ and $\boldsymbol{H}$ are turned off. This result also provides the feasibility of nonvolatile NDD switching by tuning the ME-cooled spin frozen state. In fact, the magnitude of NDD strongly depends on the cooling magnetic field (see Fig. S1 in Supplemental Material [34]). Such a behavior is qualitatively consistent with that observed for $\alpha_{xy}$ (and $\alpha_{yx}$) for a static linear ME effect which strongly depends on the cooling magnetic field [31].

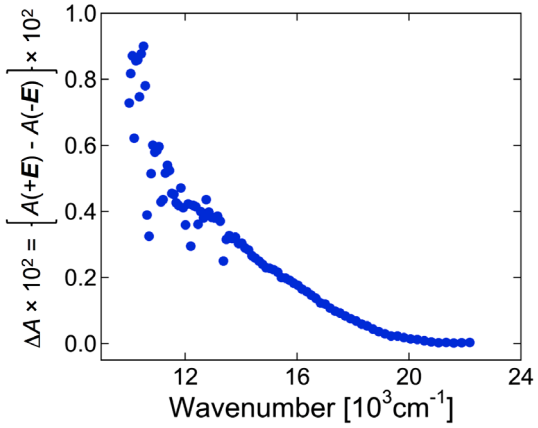


FIG. 5. Nonreciprocal directional dichroism measured with unpolarized incident light in $Ni_{0.4}Mn_{0.6}TiO_3$. The difference between the absorption spectra measured at opposite electric fields $(\pm \boldsymbol{E} = \pm 0.4\ \mathrm{MV\,m^{-1}})$, $\Delta A\{= [A(+\boldsymbol{E}) - A(-\boldsymbol{E})]\}$. The measurements were done at 4.2 K and 14 T after magnetoelectric cooling.

From the point of view of the OME effect, NDD in the present experimental configuration after the ME cooling at crossed $\boldsymbol{E}$ and $\boldsymbol{H}$ appears when a medium has finite off-diagonal elements $\alpha_{xy}$ and $\alpha_{yx}$ of the ME tensor. Here, $\boldsymbol{k}$ is along the [001] direction. The off-diagonal ME tensor can be decomposed into a sum of antisymmetric and symmetric components:

$$\begin{pmatrix} 0 & \alpha_{\mathrm{xy}} & 0 \\ \alpha_{\mathrm{yx}} & 0 & 0 \\ 0 & 0 & 0 \end{pmatrix} = \begin{pmatrix} 0 & \alpha_{\mathrm{A}} & 0 \\ -\alpha_{\mathrm{A}} & 0 & 0 \\ 0 & 0 & 0 \end{pmatrix} + \begin{pmatrix} 0 & \alpha_{\mathrm{S}} & 0 \\ \alpha_{\mathrm{S}} & 0 & 0 \\ 0 & 0 & 0 \end{pmatrix}. \tag{1}$$

The antisymmetric component $\tilde{\alpha}_A$ originates from magnetic toroidal moment $\boldsymbol{t}$ along [001] [e.g., Fig. 1(a)] while the symmetric component $\tilde{\alpha}_S$ is ascribed to a magnetic quadrupole moment $q_{xy}$ [e.g., Fig. 1(b)] [21,36,37]. The former is intact under a coordinate rotation about the $z$ axis by an arbitrary angle while the latter changes its sign under the $\pi/2$ rotation. Therefore, NDD ascribed to $\tilde{\alpha}_A$, i.e., $\boldsymbol{t}$, will appear irrespective of the polarization state of the light [6]. By contrast, the sign of NDD ascribed to $\tilde{\alpha}_S$, i.e., $q_{xy}$, is reversed by the $\pi/2$ rotation of the light polarization, and therefore NDD due to $\tilde{\alpha}_S$ disappears when the light is unpolarized. Thus, by measuring the light polarization dependence of NDD, the contribution from the respective moments can be clarified. (The possibility of polarization rotation accompanied with the propagation of the electromagnetic wave along the [001] direction is detailed in Supplemental Material [34].)

Figure 5 shows $\Delta A$ obtained by illuminating unpolarized light. The most important feature is that finite $\Delta A$ is observed in unpolarized light. This result shows that

magnetic toroidal moment contributes to the observed NDD. In other words, a spin arrangement in the ME-cooled spin glass state of NMTO includes the components of a spin texture generating the $t_z$-type toroidal moment, which is consistent with the claim of the previous Letter on the static ME effect [30]. Note that, in principle, the contribution of $q_{xy}$-type magnetic quadrupole moment can also be estimated by investigating the polarization-direction dependence of NDD with linearly polarized light. However, our present experimental accuracy is not sufficient to discuss small differences in NDD for different polarization configurations. The problem will be overcome by the improvement of the experimental setup and/or the development of glassy states with larger ME couplings in future work.

In summary, the present Letter demonstrated nonreciprocal directional dichroism originating from magnetic toroidal moments in a spin frozen state without long-range magnetic order. Furthermore, if measurements of light polarization dependence with high accuracy is carried out, the contribution of magnetic quadrupole moments to nonreciprocal optical responses can be deduced. In other words, measurements of the nonreciprocal optical responses can be a powerful tool to detect the presence of magnetoelectric multipole moments. From the symmetry point of view, not only the light propagation but also the propagation of electron and acoustic or spin wave is possible to be nonreciprocal by these multipole moments. Thus, new ways to control the various kinds of particle or quasiparticle currents in matter will be opened up.

We are grateful to N. Abe, K. Kimura, and Y. Araya for valuable discussions. This work was performed at the High Field Laboratory for Superconducting Materials, Institute for Materials Research, Tohoku University (Project No. 16H0210) and was in part supported by the Grant-in-Aid for JSPS Fellows (No. 26·8161) and JSPS KAKENHI Grants (No. JP21H01029, No. JP19H05823, No. JP21H04436, and No. 22H00101).

[1] L. D. Barron, *Molecular Light Scattering and Optical Activity*, 2nd ed. (Cambridge University Press, Cambridge, England, 2004).
[2] C. E. Rüter, K. G. Makris, R. El-Ganainy, D. N. Christodoulides, M. Segev, and D. K. Rüter, Nat. Phys. **6**, 192 (2010).
[3] L. Feng, M. Ayache, J. Huang, Y. Xu, M. Lu, Y. Chen, Y. Fainman, and A. Scherer, Science **333**, 729 (2011).
[4] B. Peng, Ş. K. Özdemir, F. Lei, F. Monifi, M. Gianfreda, G. L. Long, S. Fan, F. Nori, C. M. Bender, and L. Yang, Nat. Phys. **10**, 394 (2014).
[5] T. Arima, J. Phys. Condens. Matter **20**, 434211 (2008).
[6] D. Szaller, S. Bordács, and I. Kézsmárki, Phys. Rev. B **87**, 014421 (2013).
[7] S. Toyoda, N. Abe, S. Kimura, Y. H. Matsuda, T. Nomura, A. Ikeda, S. Takeyama, and T. Arima, Phys. Rev. Lett. **115**, 267207 (2015).
[8] S.-W. Cheong, D. Talbayev, V. Kiryukhin, and A. Saxena, npj Quantum Mater. **3**, 19 (2018).
[9] G. L. J. A. Rikken, C. Strohm, and P. Wyder, Phys. Rev. Lett. **89**, 133005 (2002).
[10] G. L. J. A. Rikken and P. Wyder, Phys. Rev. Lett. **94**, 016601 (2005).
[11] J. J. Hopfield and D. G. Thomas, Phys. Rev. Lett. **4**, 357 (1960).
[12] Y. Shimada, M. Matsubara, Y. Kaneko, J. P. He, and Y. Tokura, Appl. Phys. Lett. **89**, 101112 (2006).
[13] S. Yu, B. Gao, J. W. Kim, S. Cheong, M. K. L. Man, J. Madéo, K. M. Dani, and D. Talbayev, Phys. Rev. Lett. **120**, 037601 (2018).
[14] M. Saito, K. Taniguchi, and T. Arima, J. Phys. Soc. Jpn. **77**, 013705 (2008).
[15] I. Kézsmárki, N. Kida, H. Murakawa, S. Bordács, Y. Onose, and Y. Tokura, Phys. Rev. Lett. **106**, 057403 (2011).
[16] Y. Takahashi, R. Shimano, Y. Kaneko, H. Murakawa, and Y Tokura, Nat. Phys. **8**, 121 (2012).
[17] M. Kubota, T. Arima, Y. Kaneko, J. P. He, X. Z. Yu, and Y. Tokura, Phys. Rev. Lett. **92**, 137401 (2004).
[18] J.-H. Jung, M. Matsubara, T. Arima, J. P. He, Y. Kaneko, and Y. Tokura, Phys. Rev. Lett. **93**, 037403 (2004).
[19] H. Schmid, Ferroelectrics **252**, 41 (2001).
[20] B. B. Van Aken, J.-P. Rivera, H. Schmid, and M. Fiebig, Nature (London) **449**, 702 (2007).
[21] N. Spaldin, M. Fiebig, and M. Mostovoy, J. Phys. Condens. Matter **20**, 434203 (2008).
[22] N. Talebi, S. Guo, and P. A. Van Aken, Nanophotonics **7**, 93 (2018).
[23] V. Kocsis, K. Penc, T. Rõõm, U. Nagel, J. Vít, J. Romhányi, Y. Tokunaga, Y. Taguchi, Y. Tokura, I. Kézsmárki, and S. Bordács, Phys. Rev. Lett. **121**, 057601 (2018).
[24] T. Sato, N. Abe, S. Kimura, Y. Tokunaga, and T. Arima, Phys. Rev. Lett. **124**, 217402 (2020).
[25] K. Kimura, Y. Otake, and T. Kimura, Nat. Commun. **13**, 697 (2022).
[26] S. W. Lovesey and E. Balcar, Phys. Scr. **81**, 065703 (2010).
[27] K. Kimura, T. Katsuyoshi, Y. Sawada, S. Kimura, and T. Kimura, Commun. Mater. **1**, 39 (2020).
[28] A. Ito, H. Kawano, H. Yoshizawa, and K. Motoya, J. Magn. Magn. Mater. **104–107**, 1637 (1992).
[29] H. Kawano, H. Yoshizawa, A. Ito, and K. Motoya, J. Phys. Soc. Jpn. **62**, 2575 (1993).
[30] Y. Yamaguchi, T. Nakano, Y. Nozue, and T. Kimura, Phys. Rev. Lett. **108**, 057203 (2012).
[31] Y. Yamaguchi and T. Kimura, Nat. Commun. **4**, 2063 (2013).
[32] In these figures, $\boldsymbol{t}$ is derived by considering only a local spin texture on a hexagon in the honeycomb lattice with the origin at the center of the hexagon. Strictly speaking, the effect of translation must be considered to derive meaningful $\boldsymbol{t}$ contributing to macroscopic properties in crystalline materials. However, we here adopt these simplified illustrations to make it easier to image.
[33] Y. Sawada, S. Kimura, K. Watanabe, and M. Nakano, J. Low Temp. Phys. **170**, 424 (2013).

[34] See Supplemental Material at http://link.aps.org/supplemental/10.1103/PhysRevLett.129.217201 for spectra of NDD measured after the ME cooling at different magnetic fields and the possibility of polarization rotation.
[35] G. Bussière and C. Reber, J. Am. Chem. Soc. **120**, 6306 (1998).
[36] K. Kimura, P. Babkevich, M. Sera, M. Toyoda, K. Yamauchi, G. S. Tucker, J. Martius, T. Fennell, P. Manuel, D. D. Khalyavin, R. D. Johnson, T. Nakano, Y. Nozue, H. M. Rønnow, and T. Kimura, Nat. Commun. **7**, 13039 (2016).
[37] V. Kocsis, S. Bordács, Y. Tokunaga, J. Viirok, L. Peedu, T. Rõõm, U. Nagel, Y. Taguchi, Y. Tokura, and I. Kézsmárki, Phys. Rev. B **100**, 155124 (2019).